

# Development of Measurement System for Facial Physical Properties with Short-Distance Lighting

Takao Makino, Koichi Takase and Ryusuke Homma

Graduate School of Science and Technology, Chiba University, 1-33 Yayoi-cho, Inage-ku, Chiba 263-8522, Japan

Norimichi Tsumura<sup>^</sup> and Toshiya Nakaguchi<sup>^</sup>

Graduate School of Advanced Integrated Science, Chiba University, 1-33 Yayoi-cho, Inage-ku, Chiba 263-8522, Japan

Nobutoshi Ojima

Global R&D Beauty Creation, Kao Corporation, 2-1-3 Bunka, Sumida-ku, Tokyo 131-8501, Japan

Yoichi Miyake<sup>^</sup>

Research Center for Frontier Medical Engineering, Chiba University, 1-33 Yayoi-cho, Inage-ku, Chiba 263-8522, Japan

E-mail: invisible155@gmail.com

---

**Abstract.** *In this research, the authors have developed a compact and fast measurement system for three-dimensional (3D) shape, normal vector, and bidirectional reflectance distribution function (BRDF) of a 3D object, e.g., a human face. Since the proposed system uses linear light sources and a luminous intensity distribution of these light sources, the BRDF can be measured for a short time and without large measurement space. The proposed system is evaluated by two methods whereby the authors confirmed its accuracy: by measuring sample known objects and by comparing actual and reproduced images.*

© 2009 Society for Imaging Science and Technology.

[DOI: 10.2352/J.ImagingSci.Technol.2009.53.6.060501]

---

## INTRODUCTION

It is very important to create a realistic human face with computer graphics since such a face can be used for various applications, e.g., filmmaking, video games, or virtual cosmetics. To create the realistic facial image, it is necessary to measure facial physical parameters, i.e., the three-dimensional (3D) shape, normal vectors, and the bidirectional reflectance distribution function (BRDF) of the face. These parameters can be used for modeling the facial shape and reproducing the face under a various lighting conditions. Especially, the lighting reproduction on the face is important since the appearance of the face is changed drastically by the lighting condition. Therefore an accurate measurement system for obtaining facial physical parameters is required for realistically reproducing the human face.

Numerous measurement systems have been proposed

for obtaining accurate facial physical parameters. Most conventional systems require a very large measurement apparatus since parallel light is simply assumed for the measurement, and the light source is kept distant from the face in order to uphold this assumption. Therefore these systems do not have portability and cannot be used in a small space such as a virtual cosmetic system in a store.

In this article, we propose a compact measurement apparatus for obtaining facial physical parameters. By taking into account the luminous intensity distribution of the light sources, the various physical parameters of the face can be measured from a short distance. This system has two advantages: it is highly portable; and it can be used in a small space. In addition, we can use measured facial physical parameters to reproduce photographs of real human faces. We confirmed that the reproduced facial images have approximately same appearance of the real faces.

## RELATED WORK

Numerous approaches have been proposed for reproducing the facial appearance with measured facial physical parameters. These approaches are based on capturing the geometry of the object and calculating the BRDF at each point on the geometry. In this section, we briefly review representative works as background to our contribution.

Some conventional works use a range scanner to capture the geometry, i.e., 3D shape and normal vectors of the face. Marschner et al.<sup>1</sup> captured the geometry with the range scanner, and captured the spatially varying albedo texture using polarizing filters in front of the camera and lights to avoid specular reflection from the object. Such a polarizing technique is useful for separating specular and diffuse components of reflection, and we also used a similar technique

---

<sup>^</sup>IS&T Member.

Received Jul. 11, 2008; accepted for publication Jul. 13, 2009; published online Oct. 12, 2009.

1062-3701/2009/53(6)/060501/9/\$20.00.

to capture only the diffuse reflectance images. Weyrich et al.<sup>2</sup> also used a commercial 3D face scanner for obtaining 3D geometry of the face, and the obtained 3D geometry was used to estimate other facial properties. However, these methods have a problem that the range scanner is very expensive. An expensive measurement system is undesirable for many applications.

Another frequently used approach for capturing facial geometry involves using a multicamera system. Such an approach has an advantage that the system is inexpensive. Guenter et al.<sup>3</sup> used six camera views and reconstructed the geometry based on the dot correspondence on the face, and created texture maps for every frame of the animation. Pighin et al.<sup>4</sup> reconstructed the 3D model with several facial images from different viewpoints. They also proposed to re-synthesize facial animation through 3D model-based tracking and performed facial reproduction. These measurement methods with the multicamera system can obtain a 3D facial model inexpensively, but they also need an operation to find corresponding points among images captured by the multicamera method. This operation is typically difficult and requires a long time to calculate the result.

We therefore use a structured light method<sup>5</sup> for obtaining the 3D facial shape. The structured light method<sup>5</sup> is known as a 3D measurement method which does not use the corresponding points. It is a triangulation method which uses a single camera and a single projector. We can obtain the facial 3D shape easily and inexpensively using this method, but the obtained 3D shape does not include the high spatial frequency components. Zhang et al.<sup>6</sup> captured high spatial frequency components of the 3D shape using both the multicamera system and projectors. However, if we use many projectors and cameras, the measurement system will get complex. In our method, we use only one camera and one projector to obtain the low spatial frequency components of the 3D facial shape. High spatial frequency components are then obtained using photometric stereo method.<sup>7</sup>

The photometric stereo method<sup>7</sup> is known as the method for estimating normal vectors of the subject using images illuminated from various directions. In our method, normal vectors thus obtained are used to provide high spatial frequency information on the 3D shape. Normally, photometric stereo method needs long-distance light sources for illuminating the subject. Such a long-distance light source makes the measurement system larger. We solve this problem by considering the luminous intensity distribution of light sources; luminous intensity distribution is also used in measuring the facial BRDFs.

Next, we will review the measurement method for the facial BRDFs. For measuring the BRDF of the face, many conventional approaches need many images taken under various directional lights. Debevec et al.<sup>8</sup> proposed a lighting system for various directional lights (light stage) and saved the images as relightable 3D face models. This system requires a very large lighting apparatus, and the subject is accordingly illuminated from various directions. BRDF of the

subject is then obtained from the captured images. Hawkins et al.<sup>9</sup> extended the technique for variations in lighting for facial expressions, Wenger et al.<sup>10</sup> achieved 3D face video using very high speed cameras to capture many images under various directions of illumination within 1/30 s. Einarsson et al.<sup>11</sup> extended this approach to record human locomotion. These techniques are used in the film industry for postproduction to create realistic compositions between the human face and environmental illuminants. Recently, appearance capturing that is highly accurate<sup>2</sup> has been achieved for realistic facial synthesis. However, these methods require measurement apparatus that are large, complex, or expensive. Such apparatus are difficult to use in many practical applications.

On the other hand, the BRDF of the subject may be approximated using a BRDF reflectance model, e.g., Phong model or Torrance-Sparrow model. The model can be used as an approximate BRDF by estimating unknown parameters of the model from images taken under various directional light sources. This method can reduce the number of captured images compared to the methods reviewed above. However, even this method still needs the large measurement apparatus for capturing images. Takase et al.<sup>12</sup> proposed a compact measurement system by considering luminous intensity distribution of the light sources. In this article, we improve on their method and apply it to the facial BRDF measurement.

## COMPACT MEASUREMENT APPARATUS

In this section, we describe the compact face measurement system, the advanced light box. Figure 1 shows the flow of the process for obtaining the facial physical parameters. These parameters are obtained with three sets of images captured from the proposed apparatus, such as images projected using a structured light pattern from a projector, images illuminated by nine light-emitting diodes (LEDs,) and images captured with two shutter speeds under illumination by linear light sources. This processing workflow shares large parts with the image processing workflow of Weyrich et al.<sup>2</sup> Unlike their image processing, we use the projector instead of a face scanning system and take into account the luminous intensity distribution. Our advanced light box is described first, estimation of the facial shape and normals is then described, and finally we treat the facial BRDF estimation.

### Advanced Light Box

The advanced light box used to capture the set of images is shown in Figure 2(a). The subject sits on the chair with a headrest. One video camera takes the face from a distance of approximately 0.8 m. We are using a color digital camera (Sony DFW-X710) with a 1024×768 charge coupled device sensor. The advanced light box has three types of light sources: the projector (Toshiba TDP-FF1 Ultra Portable LED Projector), nine LEDs (Lumileds LXHL-LW6C White 5W Star LEDs), and two linear light sources (National FHL10EX-W fluorescents). The projector and LEDs are used to obtain the 3D shape and normals, and the linear light

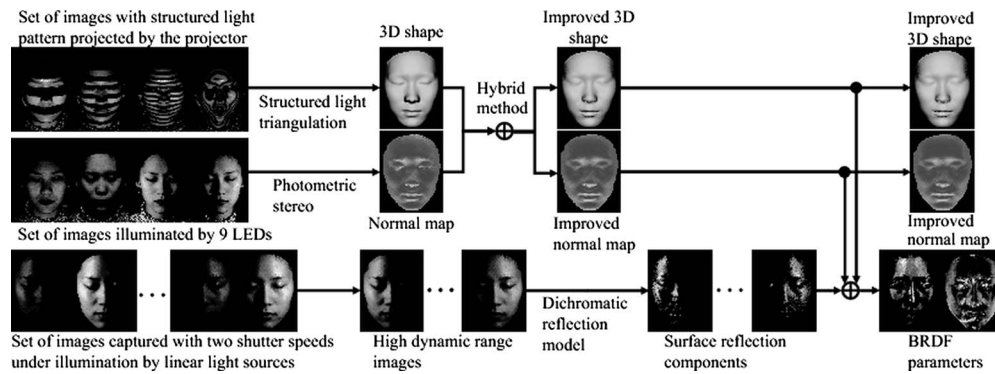


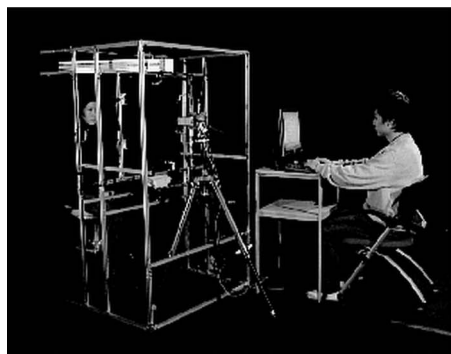
Figure 1. Workflow for measurement with the advanced light box.

sources are used to obtain the BRDF. Figs. 2(b) and 2(c) show the geometry of the advanced light box from the side and top, respectively. It takes 90 s to capture all the required images.

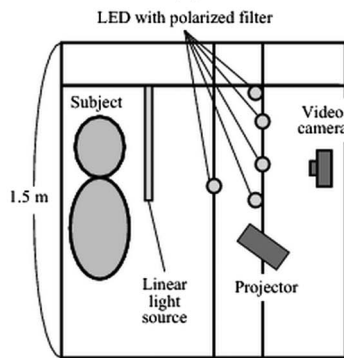
We calibrate the white balance of the camera by taking a diffuse white board illuminated by the linear light sources. The calibration of intrinsic and extrinsic camera parameters is performed by the method of using a calibration object whose 3D geometry is known.<sup>13</sup> The calibration between the camera and the projector is also performed with the same method as used by Valkenburg and McIvor.<sup>5</sup>

All light sources are within 1 m from the subject. The width, height, and depth of the advanced light box are approximately 0.9, 1.5, and 1.2 m, respectively. These sizes are very small, and we can construct this geometry with a small number of building components compared to conventional systems.<sup>2,8,10</sup> For example, the previous systems needed a subdivided icosahedron more than 2 m in diameter and more than 150 individual light sources.<sup>2,10</sup> In addition, they needed special equipment, e.g., a commercial face scanning system<sup>2</sup> or a high-speed digital camera.<sup>10</sup> However, our advanced light box has less than half the volume of the previous systems and consists of only 11 light sources and one projector with two linear stages (Oriental Motor EZS6E085-K motorized linear slides) for moving the linear light sources to control the luminous intensity distribution<sup>12,14</sup> of the light sources as described below.

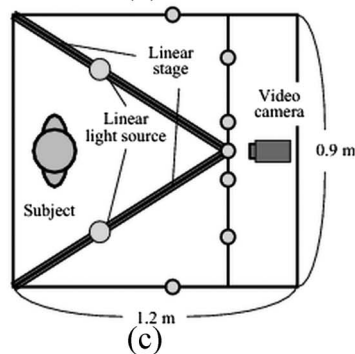
The luminous intensity distribution of the linear light source<sup>12</sup> was used to measure the BRDF. The luminous intensity distribution characterizes the radiance of the light sources. Generally, in the BRDF measurement, distant light sources are used as directional light sources as shown in Figure 3(a). However, use of the information on the luminous intensity distribution makes possible measurement of BRDF with short-distance light sources, as shown in Fig. 3(b). We use the luminous intensity distribution of the linear light sources as shown in Fig. 3(c). Since the linear light sources can illuminate the subject simply by linear motion as shown in Fig. 3(e), then the BRDF can be obtained efficiently.<sup>15</sup> On the other hand the conventional measurement system<sup>12</sup> cannot measure the side of the subject because it has only one linear light source. Therefore our measurement system has two linear light sources in order to



(a)



(b)



(c)

Figure 2. (a) Geometry of our advanced light box. (b) Illustrations of the side view and (c) top view of the advanced light box. The projector and LEDs are used for obtaining the 3D shape and normals, and the linear light sources are used for obtaining the BRDF.

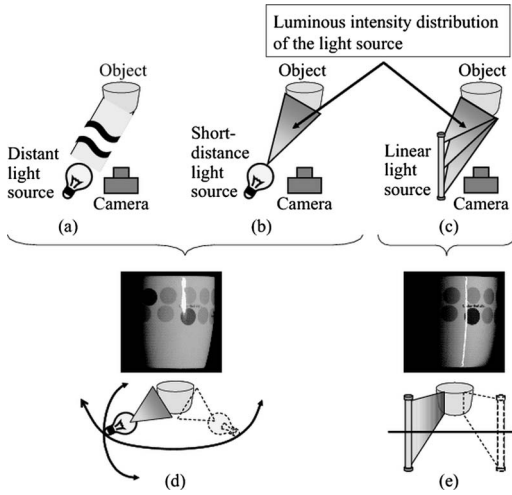


Figure 3. A point light source must be set at the distant point from the subject to make the incident light parallel. (b) A point light source or (c) a linear light source can be used in the short distance by taking into account the luminous intensity distribution. In case (d) which uses the point light source, the light source needs to move through various angles to measure the subject's whole surface. In case (e) which uses the linear light source, the light source needs to move only by linear motion.

illuminate the large area of the subject as shown in Fig. 2(c). In addition, we can measure the normal vectors with LEDs placed at short distance from the face by considering the luminous intensity distribution of the LEDs.

### Measuring Facial 3D Shape and Normal Vectors

Facial 3D shape and normal vectors can be estimated from images illuminated by the projector and LEDs. The projector casts a coded pattern onto the face from a distance of approximately 1 m, while the video camera is capturing the images. The captured images are used in the coded structured light technique<sup>5</sup> for reconstructing the facial 3D shape. The LEDs with a polarizing filter illuminate the face from various directions, and the polarizing filter is also set in front of the video camera for removing specular reflection. From the diffuse reflection images, the normal vectors are obtained by the photometric stereo method.<sup>7</sup> The conventional photometric stereo method needs to keep the light distant from the subject to accommodate the assumption of parallel light. Luminous intensity and directions can be equalized over all measurement points of the subject on the basis of this assumption. However, we have to apply the photometric stereo method with LEDs at a short distance from the subject. Therefore we consider the luminous intensity distribution of the LEDs and the measured facial 3D shape to set the viewing and illumination angles accurately.

Figure 4 shows the schematic illustration of our photometric stereo method with LEDs at a short-distance from the subject. First, we assume that the LED's luminous intensity distribution is the same as that of a point light source. In this case, the pixel value  $I$  at the Lambertian measurement point  $p$  is defined as follows:

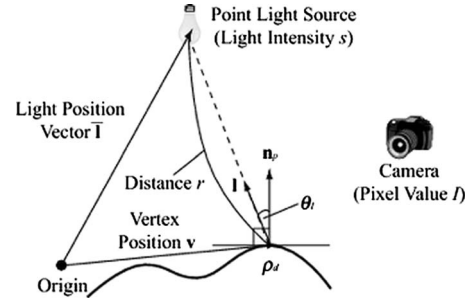


Figure 4. Schematic illustration of our photometric stereo method with LEDs at a short distance from the subject.

$$I = \rho_d \frac{s}{r^2} (\mathbf{l}^T \cdot \mathbf{n}_p), \quad (1)$$

where  $\rho_d$  is the diffuse reflectance at the measurement point,  $s$  is the luminous intensity,  $r$  is the distance between LED and the measurement point,  $\mathbf{l}$  is the lighting direction, and  $\mathbf{n}_p$  is the normal vector of the measurement point;  $1/r^2$  shows the attenuation of luminous intensity by the distance between LED and the measurement point and  $T$  means transposition of vectors of matrices. For obtaining these unknown parameters, we use the light position vector  $\bar{\mathbf{l}}$  and the vertex vector  $\mathbf{v}$ .  $\bar{\mathbf{l}}$  is obviously known, and  $\mathbf{v}$  can be obtained since we have already measured the facial 3D shape using the projector. We can obtain  $r$  and  $\mathbf{l}$  using  $\bar{\mathbf{l}}$  and  $\mathbf{v}$  as follows:

$$r = |\bar{\mathbf{l}} - \mathbf{v}|, \quad (2)$$

$$\mathbf{l} = \frac{\bar{\mathbf{l}} - \mathbf{v}}{r}.$$

If we capture three pixel values  $I_i (i=1,2,3)$  under different three light position  $\mathbf{l}_i$ ,  $I_i$  are defined using  $r_i$  and  $\mathbf{l}_i$  as follows:

$$\begin{pmatrix} I_1 \\ I_2 \\ I_3 \end{pmatrix} = \rho_d s \begin{pmatrix} 1/r_1^2 & 0 & 0 \\ 0 & 1/r_2^2 & 0 \\ 0 & 0 & 1/r_3^2 \end{pmatrix} \begin{pmatrix} \mathbf{l}_1^T \\ \mathbf{l}_2^T \\ \mathbf{l}_3^T \end{pmatrix} \mathbf{n}_p, \quad (3)$$

$$\mathbf{l} = \rho_d s \mathbf{R} \mathbf{L} \mathbf{n}_p.$$

Since  $\mathbf{n}_p$  has unit length,  $\mathbf{n}_p$  can be obtained as follows:

$$\mathbf{n}_p = \frac{\mathbf{R}^{-1} \mathbf{L}^{-1} \mathbf{l}}{|\mathbf{R}^{-1} \mathbf{L}^{-1} \mathbf{l}|}. \quad (4)$$

Using these equations, we can calculate facial normal vectors with short-distance LEDs from the subject. The facial 3D shape and normals are shown in Figure 5. Absolute values of  $x$ ,  $y$ , and  $z$  coordinates of the facial normals are read as  $R$ ,  $G$ , and  $B$  components of the color. The facial 3D shape and normals are used in a hybrid algorithm<sup>16</sup> for obtaining a more accurate facial 3D shape and normals.

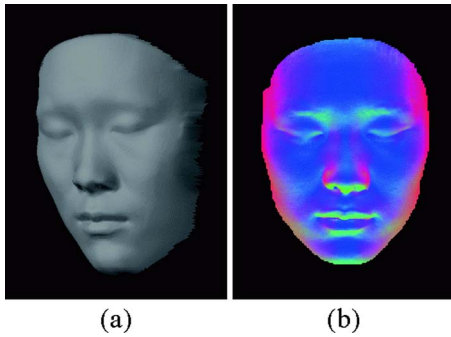


Figure 5. (a) Facial 3D shape and (b) facial normals obtained with the hybrid algorithm.

### Measuring Facial BRDF Parameters

We estimate facial BRDF parameters with images illuminated by the linear light sources. The BRDF measurement in the light box means the estimation of diffuse, specular, and surface roughness parameters of the Torrance-Sparrow model.<sup>17</sup> This model can deal with an off-specular reflection as occurs on human skin. Accordingly the Torrance-Sparrow model is found to be useful for measuring facial BRDF. However, this model is not sufficient to obtain the correct facial BRDF. We have to consider subsurface scattering<sup>2</sup> and skin layers which have different reflection properties.<sup>8</sup> In this article, we used only the Torrance-Sparrow model because the consideration of subsurface scattering and skin layers makes the measurement system more complex. This consideration is deferred to our future work.

The Torrance-Sparrow model is described as follows:

$$\rho_d = \frac{r_d}{\pi}, \quad (5)$$

$$\rho_s(p, \omega_o, \omega_i) = r_s \frac{D(\omega_h, \sigma)G(\omega_o, \omega_i)F(\omega_o)}{4 \cos \theta_o \cos \theta_i}, \quad (6)$$

where  $\rho_d$  and  $\rho_s$  are the diffuse and the specular reflectance,  $r_d$  and  $r_s$  represent the diffuse and the specular parameters, respectively, and  $(\omega_o; \omega_i)$  denotes a pair of directions from a surface point  $p$  to a light source and a viewer, respectively;  $(\theta_o; \theta_i)$  shows a pair of angles between a surface normal and  $\omega_o$ , a surface normal and  $\omega_i$ , respectively. In the Torrance-Sparrow reflectance model,  $D$ ,  $G$ , and  $F$  denote a microfacet distribution, a geometric attenuation term, and Fresnel reflection, respectively, and  $\omega_h$  is a half vector between  $\omega_o$  and  $\omega_i$ ;  $\sigma$  represents surface roughness. The parameters  $(r_d; r_s; \sigma)$  were estimated at each pixel on the acquired image by a least-squares fitting operation.

For the fitting operation, we use images illuminated by the linear light sources. The linear light sources, whose luminous intensity distribution is measured, are moved linearly using the linear stage while these light sources illuminate the face. The video camera captures the face image at each position of the linear light sources at two different shutter speeds to produce a high dynamic range image.

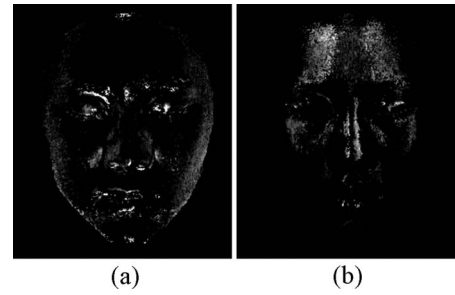


Figure 6. Obtained BRDF parameters. (a) Specular parameter and (b) surface roughness.

Three steps are necessary for obtaining the BRDF. The processing is same as in Takase's method.<sup>12</sup> First, high dynamic range images are produced from the two images captured at different shutter speeds.<sup>18</sup> Second, the high dynamic range images are separated into diffuse and specular reflection images using the dichromatic reflection model.<sup>19</sup> We have already obtained diffuse reflection images illuminated by LEDs with the polarizing filter. However, we need both diffuse and specular reflection images illuminated by the linear light sources, and the polarizing filter method cannot obtain diffuse and specular reflection images at the same time. We solve these problems using the method of the dichromatic reflection model method. Separate images are separated again into unit color vectors and intensity at each pixel.<sup>20</sup> We do not have to estimate the BRDF parameter of each color channel because color information is separated in this processing. Intensities are used to obtain BRDF parameters in the next processing step.

Finally, the BRDFs are calculated by fitting the BRDF model (Torrance-Sparrow model<sup>17</sup>) with consideration of the luminous intensity distribution. Takase et al.<sup>12</sup> proposed the method that can estimate BRDF parameters from images illuminated by a linear light source with a known luminance intensity distribution. In general, a linear light source cannot be used for measurement because it illuminates the subject redundantly from various angles of incidence along the longitudinal direction. In Takase's method, it is assumed that the linear light source is composed of many point light sources. The contribution of each of the point light sources to the reflection is calculated independently. This enables the BRDF parameter measurement with the linear light source. We can obtain facial BRDF parameters, diffuse parameters, specular parameters, and surface roughness by applying this method to the human face. Figure 6 shows specular parameter and surface roughness at each pixel. Note that Fig. 6(a) shows the value of the specular reflectance parameter at each pixel not the specular reflection component.

### EXPERIMENTAL EVALUATION FOR THE PROPOSED MEASUREMENT SYSTEM

In this section, the application of the light box is evaluated experimentally. First, we evaluate the accuracy of the measured parameters, 3D shape, normal vectors, and BRDF. We then evaluate the reproduced human faces derived from the measured facial physical parameters by comparing them to real human faces.

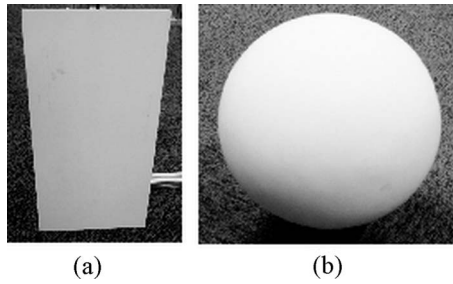


Figure 7. Subjects used in the experimental 3D shape evaluation. (a) Board and (b) spherical object.

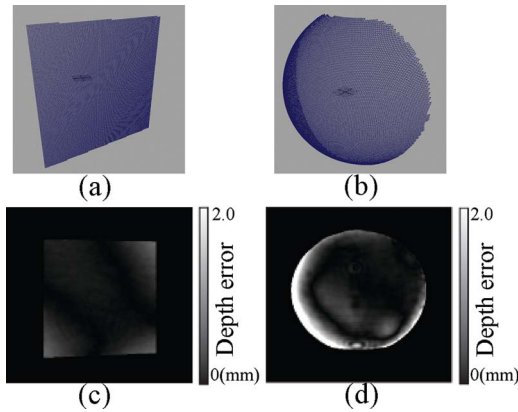


Figure 8. Measured 3D shape of (a) the board and (b) spherical object; [(c) and (d)] corresponding errors between measured 3D shape and ground truth shape.

Table I. RMSE and maximum error of measured 3D shape of two subjects.

	Board	Sphere
RMSE(mm)	0.24	1.09
Maximum error(mm)	0.91	5.78

### Experimental Evaluation for 3D Shape and Normals

First of all, we measure the 3D shape of two subjects and compare them to ground truth shape. Subjects of this experiment are board and spherical objects as shown in Figure 7. We wanted to use a real human face as the subject, but it is difficult to obtain the ground truth shape of human faces. Therefore we used these simple objects since their ground truth shape can be obtained easily and accurately. Figures 8(a) and 8(b) show the measured 3D shape of two subjects, and Figs. 8(c) and 8(d) show errors between measured 3D shape and ground truth shape. Table I shows root mean square error (RMSE) and maximum error calculated from Figs. 8(c) and 8(d). The RMSE of the board is 0.24 mm and the RMSE of the spherical object is 0.91 mm, respectively. These results show that the light box can obtain the 3D shape of the board and the spherical object with reasonably high accuracy. However, there are large errors, up to 5.78 mm, at the left side of the sphere. We think these errors have been observed because points on the side of the sphere were

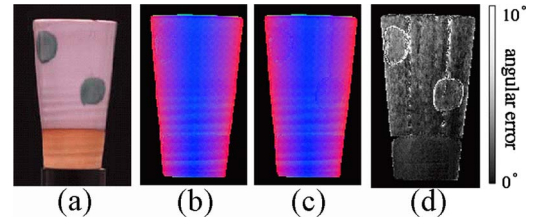


Figure 9. (a) Subject; (b) normals measured by the proposed method; (c) normals measured by the conventional method; (d) error map image.

Table II. RMSE and maximum error of measured normal vectors by two methods.

	Error between proposed and conventional methods
RMSE (deg)	1.81
Maximum error (deg)	9.86

not illuminated sufficiently by rays from the LEDs and the projector. From these results, we can say that our system can measure the 3D shape of the measured object in the frontal region.

Then we compare measured normal vectors to ground truth normals. We use a cup, shown in Figure 9(a), as a subject for this comparison. This subject has both high and low spatial frequency components. Using this subject, we can confirm the accuracy of our measurement for both high and low spatial frequency normals. First, we obtain ground truth vectors of the subject. We measure normal vectors by the conventional photometric stereo method instead of our short-distance photometric stereo method, and measured normals are used as ground truth normals in this experiment. Next, we obtain normal vectors using the proposed short-distance photometric stereo method. Finally, these two measurement results are compared. Figs. 9(b) and 9(c) show normals measured by our method and ground truth, respectively. Absolute values of  $x$ ,  $y$ , and  $z$  coordinates of subject normals are read as  $R$ ,  $G$ , and  $B$  components of the color. Fig. 9(d) shows the error between Figs. 9(b) and 9(c), and Table II shows RMSE and maximum error calculated from Fig. 9(d). These results show that our short-distance photometric stereo method can measure normals with same level of accuracy as the conventional photometric stereo method. The maximum error is  $9.86^\circ$  and this is a very large difference. However, we think this maximum error is not serious problem because this error only occurs at the boundary with the background.

### Experimental Evaluation for BRDF

In this experiment, we measure BRDF parameters of two subjects and compare them to ground truth BRDF parameters. Subjects of this experiment are two skin replicas with different colors shown in Figure 10. These replicas are made of skinlike material; their BRDF parameters are known, so we can use them as ground truth. So we can use their BRDF parameters as ground truth.

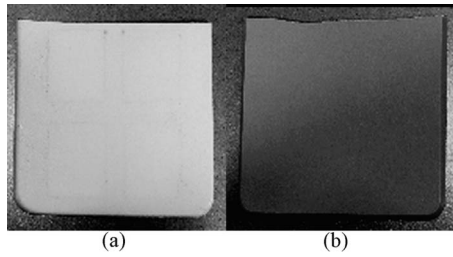


Figure 10. Two skin replicas used in the experimental BRDF evaluation. (a) Skin replica 1 and (b) skin replica 2.

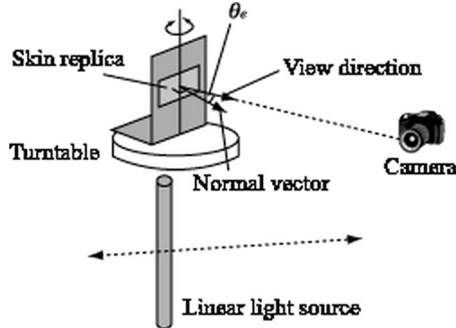


Figure 11. Schematic illustration of BRDF measurement from various viewing directions.

The light box measures BRDF parameters from only one viewing direction. If the angle between normal vectors and viewing direction vectors is changed, the light box may not measure BRDF parameters correctly. Therefore, we compare BRDF parameters measured from various viewing directions. Figure 11 shows the schematic illustration of this measurement. The motorized turntable rotates the subject  $0^\circ$ – $60^\circ$  by  $5^\circ$  increments, and BRDF parameters are measured at each angle.

Table III shows average and maximum error between ground truth and measured BRDF parameters, and Figure 12 shows results of comparing the measured BRDF parameters to ground truth. Note that Fig. 12 shows values of BRDF parameters not actual reflectance of the subject. These results show that the light box can obtain diffuse parameters and surface roughness of the skin replica with an inaccuracy of less than 10%. Table III and Fig. 12 also show that the specular parameter has the higher error than other parameters. It is considered that the specular parameter is sensitive to changes in the viewing angle. We think these measurement errors are not large, but these errors may make serious difference on the facial image reproduction. We evaluate

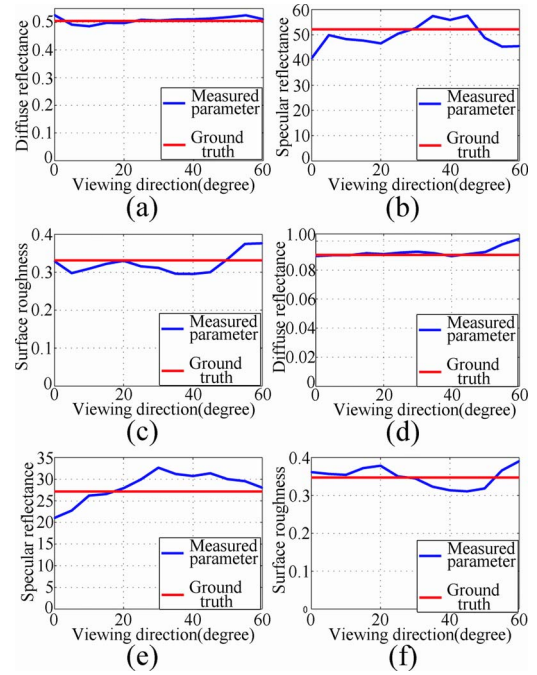


Figure 12. Comparison of measured BRDFs with ground truth BRDFs (diffuse and specular parameter-mean parameters of the Torrance-Sparrow model, not actual reflectance); [(a)–(c)] Skin replica 1 and [(d)–(f)] skin replica 2.

measured BRDF parameters using reproduced facial images in the next subsection. In addition, we think the color of the replica has little effect on the accuracy of BRDF measurement.

### Reproduced Image Evaluation

In this experiment, we compare reproduced facial images to real facial photographs and evaluate the accuracy of reproduced images. First, we measure the facial physical parameters of a subject with the light box. Then, we reproduce the facial image of the subject with measured facial physical parameters. Figures 13(a) and 13(c) show real facial photographs of two subjects and Figs. 13(b) and 13(d) show reproduced facial images. They have a strong resemblance to each other in shape and color. As another example, Figure 14 shows real facial photographs and reproduced facial images under different lighting directions and viewing directions. While these reproduced images have a few differences from the real photographs, the appearance of these images is very similar to the appearance of real photographs. From these results, we infer that the measured facial physical parameters incorporate sufficiently accurate information to reproduce the facial image.

Table III. Average and maximum error of measured BRDF parameters(%).

	Surface replica 1			Surface replica 2		
	Diffuse parameter	Specular parameter	Surface roughness	Diffuse parameter	Specular parameter	Surface roughness
Average error	2.31	9.92	7.51	2.52	11.09	6.14
Maximum error	5.29	23.33	12.61	12.24	22.53	12.38

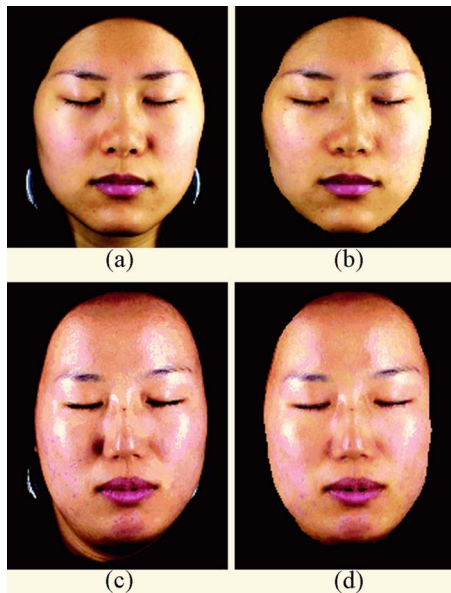


Figure 13. [(a) and (c)] Real facial photographs and [(b) and (d)] reproduced facial images based on measured facial physical properties.

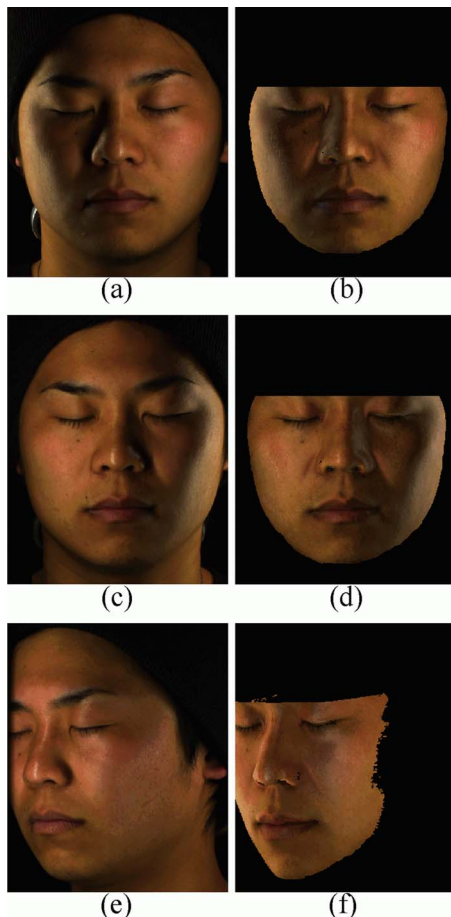


Figure 14. [(a), (c), and (e)] Real facial photographs and [(b), (d), and (f)] reproduced facial images from different lighting and viewing direction.

## DISCUSSION AND CONCLUSIONS

In this article, we have proposed the advanced light box, which is a compact measurement apparatus for obtaining facial physical parameters. Using the advanced light box, we could obtain the 3D shape, normal vectors, and BRDFs of the face without an apparatus occupying a large space. Experiments showed that the facial physical parameters can be measured using the developed system with small errors. These facial physical parameters were used for reproducing photographs of real human faces. We compared real facial images to the resultant images, and the results showed that both images have a strong resemblance each other.

In future work, the advanced light box could be improved for more accurate and comfortable measurement. Especially, the improvement of 3D shape measurement error is one of the most important problems to be solved. Our advanced light box has two linear light sources which are moved along linear stages. If we can move the linear light sources along the face in a circular trajectory, we will obtain more accurate BRDFs of the entire face and can make the advanced light box smaller and simpler.

We have evaluated measured BRDF parameters, but this evaluation is empirical. We have to research how small a BRDF error is necessary to enable us to reproduce the appearance of the object. Therefore it will be necessary to confirm accurate measurement of BRDF in order to reproduce the appearance of the 3D object. In addition, we need to evaluate our system and image reproduction thereby with various types of subjects, e.g., elderly people or people of various races.

In further future work, we have to consider more detail of human skin, e.g., skin layers, subsurface scattering, and anisotropic reflection characteristics. These components are important to obtain accurate reflectance properties of human skin. We have to elaborate our measurement apparatus to enable consideration of these components.

## REFERENCE

- <sup>1</sup>S. Marschner, B. Gunter, and S. Raghupathy, "Modeling and rendering for realistic facial animation", *Proceedings of Eurographics Symposium on Rendering* (Eurographics Association, Brno, 2000) pp. 231–242.
- <sup>2</sup>T. Weyrich, W. Matusik, H. Pfister, B. Bickel, C. Donner, C. Tu, J. McAndless, J. Lee, A. Ngan, and H. W. Jensen, "Analysis of human faces using a measurement-based skin reflectance model", *ACM Trans. Graphics* **25**, 1013 (2006).
- <sup>3</sup>B. Guenter, C. Grimm, D. Wood, H. Malvar, and F. Pighin, "Making faces", *Proc. SIGGRAPH 1998* (ACM Press/ACM SIGGRAPH, New York, 1998) pp. 55–66.
- <sup>4</sup>F. Pighin, R. Szeliski, and D. H. Salesin, "Resynthesizing facial animation through 3D model-based tracking", *Proc. Seventh IEEE International Conference on Computer Vision* (IEEE, Piscataway, NJ, 1999) pp. 143–150.
- <sup>5</sup>R. J. Valkenburg and A. M. McIvor, "Accurate 3D measurement using a structured light system", *Image Vis. Comput.* **16**, 99 (1998).
- <sup>6</sup>L. Zhang, N. Snavely, B. Curless, and S. M. Seitz, "Spacetime faces: High resolution capture for modeling and animation", *ACM Trans. Graphics* **23**, 548 (2004).
- <sup>7</sup>R. J. Woodham, "Photometric method for determining surface orientation from multiple images", *Opt. Eng.* **19**, 139 (1980).
- <sup>8</sup>P. Debevec, T. Hawkins, C. Tchou, H. p. Duiker, W. Sarokin, and M. Sagar, "Acquiring the reflectance field of a human face", *Proc. SIGGRAPH 2000* (ACM Press/ACM SIGGRAPH, New York, 2000) pp. 145–156.
- <sup>9</sup>T. Hawkins, A. Wenger, C. Tchou, A. Gardner, F. Goransson, and P.

- Debevec, "Animatable facial reflectance fields", *Proc. Eurographics Symposium on Rendering* (Eurographics Association, Grenoble, 2004) pp. 309–319.
- <sup>10</sup> A. Wenger, A. Gardner, C. Tchou, J. Unger, T. Hawkins, and P. Debevec, "Performance relighting and reflectance transformation with time-multiplexed illumination", *ACM Trans. Graphics* **24**, 756 (2005).
- <sup>11</sup> P. Einarsson, C.-F. Chabert, A. Jones, W.-C. Ma, B. Lamond, T. Hawkins, M. Bolas, S. Sylwan, and P. Debevec, "Relighting human locomotion with flowed reflectance fields", *Proc. Eurographics Symposium on Rendering* (Eurographics Association, Nicosia, 2006) pp. 183–194.
- <sup>12</sup> K. Takase, N. Tsumura, and Y. Miyake, "Measurement of bidirectional reflectance distribution function with a linear light source", *Opt. Rev.* **15**, 187 (2008).
- <sup>13</sup> O. Faugeras, *Three-Dimensional Computer Vision: A Geometric Viewpoint* (MIT Press, Cambridge, 1993), pp. 51–66.
- <sup>14</sup> K. Takase, N. Tsumura, T. Nakaguchi, and Y. Miyake, "Measuring light field of light source with high directional resolution using mirrored ball and pinhole camera", *Opt. Rev.* **13**, 314 (2006).
- <sup>15</sup> A. Gardner, C. Tchou, T. Hawkins, and P. Debevec, "Linear light source reflectometry", *ACM Trans. Graphics* **22**, 749 (2003).
- <sup>16</sup> D. Nehab, S. Rusinkiewicz, J. Davis, and R. Ramamoorthi, "Efficiently combining positions and normals for precise 3D geometry", *ACM Trans. Graphics* **24**, 536 (2005).
- <sup>17</sup> K. E. Torrance and E. M. Sparrow, "Theory for off-specular reflection from roughened surfaces", *J. Opt. Soc. Am.* **57**, 1105 (1967).
- <sup>18</sup> P. Debevec and J. Malik, "Recovering high dynamic range radiance maps from photographs", *Proc. SIGGRAPH 1997* (ACM Press/ACM SIGGRAPH, Los Angeles, 1997) pp. 369–378.
- <sup>19</sup> S. A. Shafer, "Using color to separate reflection components", *Color Res. Appl.* **10**, 210 (1985).
- <sup>20</sup> Y. Sato and K. Ikeuchi, "Temporal-color space analysis of reflection", *J. Opt. Soc. Am. A Opt. Image Sci. Vis.* **11**, 2990 (1994).